

# Self-organized Growth of SiGe and SiGeC Quantum Dots and Wires

J. Stangl, T. Roch, V. Holý, G. Bauer

Institut für Halbleiter-und Festkörperphysik, Johannes Kepler Universität  
A-4040 Linz, Austria

O.G. Schmidt, C. Lange, K. Eberl

Max-Planck-Institut für Festkörperforschung, D- 70569 Stuttgart, Germany

J. Zhu, K. Brunner, G. Abstreiter

Walter Schottky Institut, TU München, D- 85748 Garching, Germany

The lateral ordering, the size and shape of SiGe and SiGeC self-organized nanostructures, which were grown by molecular beam epitaxy, was investigated by grazing incidence small angle x-ray scattering and by atomic force microscopy.

## 1. Introduction

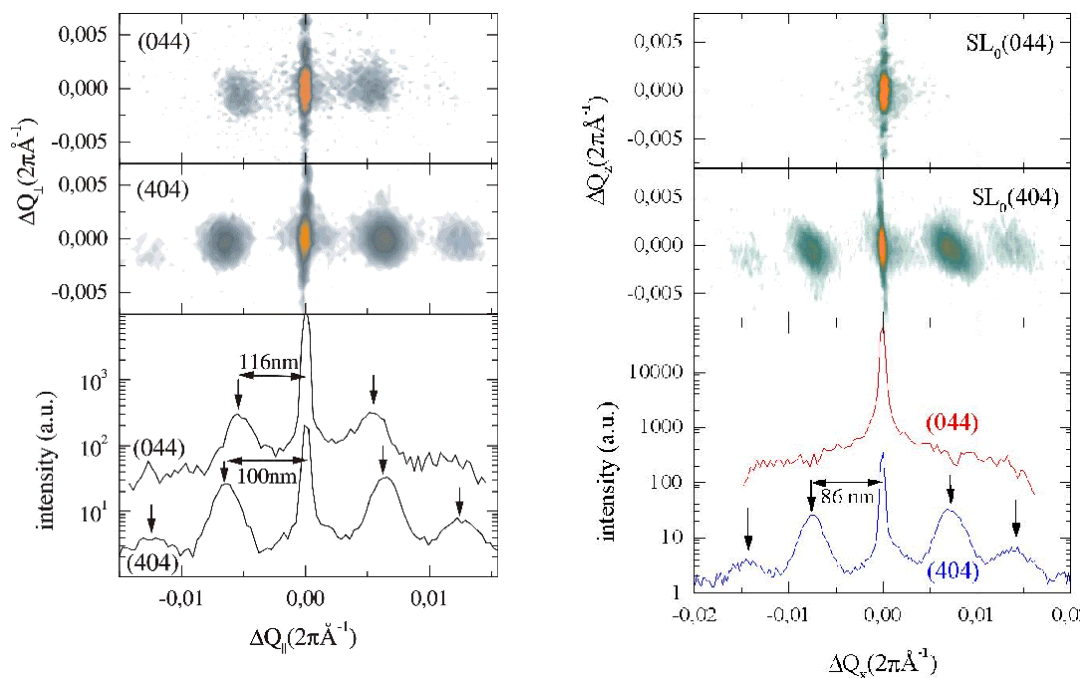
SiGe nanostructures can be realized by lateral patterning using lithography and etching or by self-organized growth. The latter method has the advantage that surface layer defects introduced by the fabrication procedure can be avoided. Its disadvantage is related to the rather broad size distribution. The FWHM of this size distribution can be diminished by depositing the self-organized nanostructures on suitable templates. This will also improve the lateral ordering. In this work Si/SiGe multilayers with high Ge contents, deposited on vicinal (miscut) Si substrates, which exhibit step-bunching, were used as templates for the subsequent growth of Ge rich islands and for wires oriented along the direction of steps. In order to achieve sufficiently small islands which exhibit three dimensional quantization effects, carbon induced islands have to be grown, which exhibit typical sizes of about 3 to 15 nm, accompanied by a much higher island density. Moreover, these carbon induced quantum GeC dots embedded in Si exhibit the *most intense* photoluminescence compared to all other Si based heterostructures.

## 2. Experimental

For improving the lateral ordering of Ge rich islands and wires on Si, we have investigated two samples of similar nominal structure, using atomic force microscopy (AFM), x-ray diffraction (XRD), and grazing incidence small angle x-ray scattering (GISAXS). Sample R826 is a 20 period Si<sub>0.55</sub>Ge<sub>0.44</sub>/Si multilayer grown by molecular beam epitaxy on (001) oriented Si substrate with a miscut of 2° towards [100] direction. Each multilayer sequence consists of 2.5 nm SiGe and 10 nm Si spacer layer. Sample R888 with the same nominal structure was grown on the vicinal (001) Si substrate with a miscut of 3.5° inclined towards [100] direction.

Furthermore we investigated buried C induced Ge quantum dot multilayers grown on (001) Si by molecular beam epitaxy. Using grazing incidence small angle x-ray scattering (GISAXS) we determined the shape, the mean radius, height, and dot distance. The dot distribution is isotropic within the (001) interfaces, and no vertical correlation of the dot positions along [001] growth direction was found.

The investigated SiGeC sample was grown by solid source molecular beam epitaxy (MBE). After deposition of 0.2 ML C, 2.4 ML Ge were deposited and subsequently a Si spacer layer of 9.6 nm. This stacking sequence was repeated 50 times. After growth the sample was annealed for ~25 min at 600 °C. Since the size of the CGe dots and their distances are of the order of about 10 and ~30 nm, respectively, the corresponding distribution of scattered intensity in reciprocal space is very broad. Therefore the conventional coplanar scattering geometry cannot be used, and we have performed measurements in noncoplanar GISAXS geometry at Troika II beamline at the ESRF.



R826

R888

Fig. 1: Reciprocal space maps of samples R826 and R888 in two azimuths around (044) and (404) reflections, along steps and perpendicularly to them, respectively. The lower panels display the intensities integrated along  $Q_{\parallel} = 0.005 \text{\AA}^{-1}$  with the average dot and wire distances indicated.

In Fig.1 x-ray diffraction reciprocal maps are shown for the Ge rich island sample (R826) and for the Ge wire sample (R888) around the (044) and the (404) reflection, around the zero-th order superlattice satellite, corresponding to the azimuth along the steps and perpendicular to them, respectively. Diffusely scattered maxima for sample R826 show the correlation of dots position, which is significantly better in the direction perpendicular to the steps. For sample R888, the subsidiary maxima along  $Q_x$  are missing. This indicates, that not ordered islands are present, but rather wires oriented along [010] direction, corresponding to the direction parallel to the steps. In the island multilayer R826, steps formed due to the bunching process lead to an alignment of buried

dots along steps. The dots distances perpendicular to the step edges are very regular correlated by the step width, whereas the dot distances along the step edges show a significantly higher spread. In the R888 sample self-organized Ge-rich wires also at the buried interfaces are laterally ordered and oriented along the direction of the steps.

AFM area scans of the topmost surface (Fig. 2 (a), (b)) show clearly the presence of self-organized islands on the surface R826 and wires on the R888 sample surface. The average wire height is about 1 nm, whereas in the sample R826 the island height is about 4 nm. Autocorrelation spectra (Fig. 2 (c), (d)) can give an estimate on the size and shape of the coherent island domain (R826).

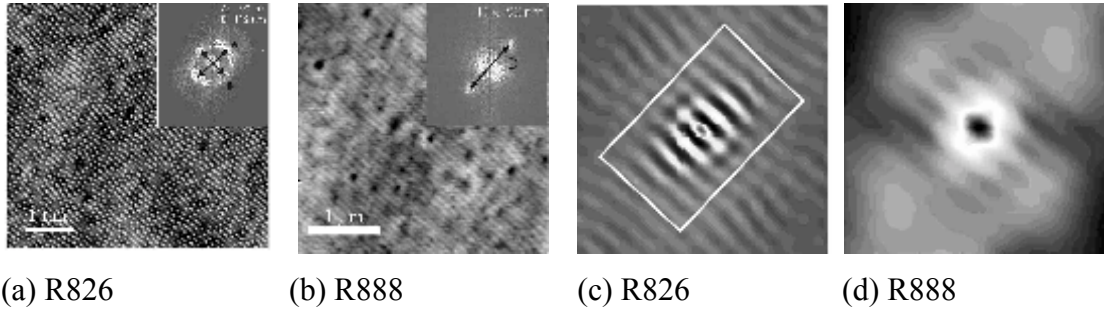


Fig. 2: AFM scans of the samples R826 (a) and R888 (b). The 2D power spectra (inset) show the mean distance of the wires. Autocorrelation spectra of samples R888 (d) and R826 (c) with the coherent dot domain (white line)  $2 \times 4$ , using a cutoff peak height of 10% of the central maximum.

The GISAXS spectra measured on the sample R826 at different azimuths are shown in Fig. 3 as a two-dimensional (2D) reciprocal space map. The 2D GISAXS data, which reflect the different ordering of the islands along the  $[100]$  and  $[010]$  directions for the buried island layers, agree very well with the surface morphology obtained by AFM. Hence in the azimuth parallel to the step edges the correlation of islands positions is significantly worse than perpendicular to the step edges.

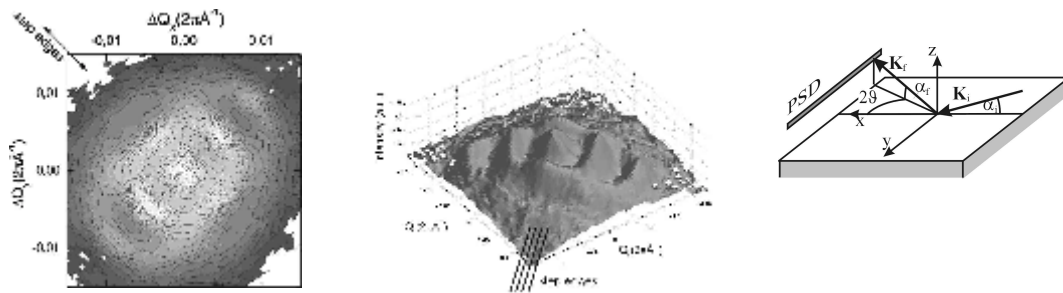


Fig. 3: GISAXS 2D map of the sample R826. The inset (right) shows the GISAXS measurement geometry, for incidence angle  $\alpha_i = 1.1^\circ$  and exit angle  $\alpha_f = 0.6^\circ$ .

The GISAXS data for the GeC dots have been evaluated using an approach known from small-angle scattering [1]. The Fourier transformation of the measured intensity curve is shown in Fig. 4 (a). The maximum of  $I^{FT}(r)$  at 30 nm corresponds to the mean distance between the dots. The region where  $I^{FT}(r)$  is negative corresponds to a zone around each of the dots where the probability of finding a neighboring dot is *smaller* than that of a

completely uncorrelated dot distribution. A good correspondence to the experimental data was found for a lens-like shape with a dot radius of  $R = (5.7 \pm 0.3)$  nm and a height of about  $h = (1.7 \pm 0.3)$  nm. These values agree reasonably well with AFM investigations of a single, uncapped CGe dot layer (see Fig. 4 (b)). From TEM investigations of the multilayer sample it is quite difficult to determine the exact dot dimensions due to the particularly large strain contrast in the CGe system. We found neither vertically nor laterally ordered dot distribution.

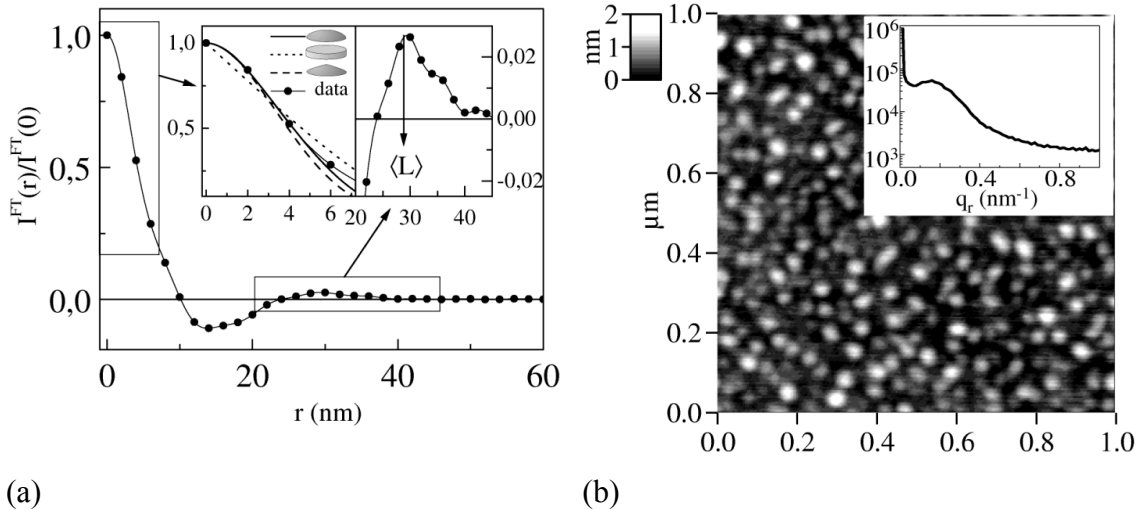


Fig. 4: (a) Fourier transformation  $I^{FT}(r)$  of the measured intensity for  $\phi = 0$  (points). The insets show the best fit to the central peak for different dot shapes (left), and an enlargement of the peak around  $r = 30$  nm, corresponding to the mean dot distance  $\langle L \rangle$  (right). (b) AFM image of a single CGe dot layer with 0.2 ML C and 3 ML Ge. The insert displays its 2D Fourier transform, integrated along the polar angle. The peak around  $q_r = 0.2 \text{ nm}^{-1}$  corresponds to the mean dot distance.

### 3. Conclusion

The structural properties of Si-based nanostructures were investigated by atomic force microscopy as well as by x-ray scattering techniques. The C induced Ge dots embedded in Si are promising for Si-based light emitting devices in the near infrared region.

### Acknowledgements

This work was supported by the FWF and the BMWV, Vienna.

### References

- [1] J. Stangl, V. Holy, P. Mikulik, G. Bauer, I. Kegel, T.H. Metzger, O.G. Schmidt, C. Lange, K. Eberl, *Appl.Phys.Lett.* **74**, 3785 - 3787 (1999).
- [2] K. Eberl, O. G. Schmidt, S. Schieker, N.Y. Jin-Philipp, And F. Philipp, *Solid State Electronics* **42**, 1593 (1998).